Indian Journal of Pure & Applied Physics
Vol. 62, June 2024, pp. 478-489
DOI: 10.56042/ijpap.v62i6.7345

Photocatalytic Activity in PVA Capped CdS/ZnS Core/Shell Nanocomposites

Pallabi Boro & Suparna Bhattacharjee*

Department of Applied Sciences, Gauhati University, Guwahati, Assam 781 014, India

Received 15 December 2023; accepted 1 May 2024

We report synthesis of PVA capped CdS/ZnS (Cadmium Sulphide/Zinc Sulphide) core/shell nanocomposites using a simple and cost effective chemical precipitation method. The synthesized samples were characterized using different characterization techniques. Results of UV-vis and PL spectroscopic analysis indicate formation of nanoparticles of CdS and CdS/ZnS whereas the XRD patterns show formation of cubic and hexagonal structure of CdS and ZnS Nanoparticles respectively. Results of TEM and SEM analysis show that, the synthesized Nanoparticles are more or less spherical in shape. The FTIR result confirms the formation of Cd-S and Zn-S bond in the CdS/ZnS core/shell structures. Results of photocatalytic study indicates that the CdS/ZnS core/shell nanocomposites shows excellent photocatalytic activity for the degradation of Methyl Orange (MO) where it was degraded nearly 83% under UV irradiation.

Keywords: XRD; SEM; FTIR; UV-vis; TEM

1 Introduction

Growing water pollution is one of the most important concerns of the present day world. Since, toxic and various hazardous compounds released from various chemical industries such as printing, dyeing, textile *etc*. finds their way into the different water bodies, located besides them; we need to find out measures which can be used to make these water bodies safe for use by all living organisms. These hazardous compounds absorb sunlight strongly which in turn affects the photosynthetic cycle of various aquatic plants thereby posing threat to the whole ecosystem. Moreover, synthetic organic dyes such as Methylene Blue, Rhodamine 6G, Methyl Orange, Congo Red *etc*., which finds use in textile, paper mills, plastic, leather etc. industries, contains chromophores in their molecular structures which makes them colourful. However, when these dyes are dispensed into lakes and other water bodies, it may cause serious health hazard, as they get transformed into toxic and carcinogenic compounds[1]. As such, researchers worldwide are trying to develop some scientific methods so that the entire globe can be made safe from such hazardous situations. Photocatalytic process is one of such methods which can contribute a lot towards environmental safety as this process can be implemented conveniently for the degradation of such dyes without the production of any secondary pollutant[1,2]. Photocatalysis is a process wherein excitons are generated in a semiconductor material by the absorption of photons having energy either more or equal to the band gap of the material. This result in excitation of the valence band electrons to the conduction band of the semiconductor and in turn causes generation of electron hole pairs[3]. The photocatalytic activity of semiconductor materials can be controlled by three factors (1) light absorption property, (2) rate of reduction and oxidation of reaction substrates by electrons and holes respectively and (3) rate of electron-hole recombination[4]. These three factors are governed by the crystal structure, surface texture and the particle size of the semiconductor nanoparticles. The morphology of the semiconductor materials depends upon the synthesis mechanism. There are several methods to synthesize CdS/ZnS nanoparticles such as co-precipitation method, solvothermal method, thermoelectrical method, sol-gel method, colloidal method *etc*[5]. Amongst the reported methods, chemical synthesis techniques are one of the most convenient and cheapest ones[6]. These different preparation methods can induce some changes in the physical and chemical properties of the synthesized nanoparticles.

Group II-VI semiconductor materials such as CdS (Cadmium Sulphide) and ZnS (Zinc Sulphide) are considered as the right photocatalysts which can show better photocatalytic activity. CdS, is susceptible to photocorrosion in long-term photocatalytic reactions

*Corresponding author:
(E-mail: suparnabhattacharjee3@gmail.com; suparna@gauhati.ac.in)

despite being able to absorb evoking light in the visible range with ease[7]. ZnS nanocrystals are also one of the most efficient photocatalysts due to their ability of quick generation of electron-hole pairs and due to the strong negative redox potentials of excited electrons. However, their photocatalytic activity under visible light, which makes up the majority of solar energy, was observed to get constrained by their wide band gap and intrinsic defects[8].

Yu *et al*. in the year 2010 showed that the cubic phase of CdS nanoparticles can show the best photocatalytic degradation activity toward Rhodamine B (RB) due to their larger ability of absorption and absorbance[9]. In 2013, Fenguang *et al*., studied the photocatalytic activity of CdS Nanoparticles. They found that CdS Nanoparticles showed excellent photocatalytic activity for the degradation of Rhodamine B under UV irradiation and degraded 95% after 60 minutes of irradiation[10]. Bhadwal *et al*., in the year 2014 found that the CdS Nanoparticles can degrade 37.15% of Methyenel Blue (MB) when the irradiation time was 60 minutes[11].

In 2012 Luo *et al*. found that ZnS hollow sub-micrometer spheres showed more photodegradation efficiency for the polluting agents such as Rhodamine B and Salicyclic acid than that of the commercial ZnS, CdS and TiO_2P_25 under visible light and also in presence of UV light[12]. Yin *et al*., in the year 2016 studied the photocatalytic degradation of methyl orange with ZnS catalyst and found that the degradation of methyl orange was 97.4% under UV light within 20 minutes[13]. Chanu *et al*., in the year 2016 synthesized and characterized ZnS nanoparticles and studied the photocatalytic activity of the same material. They found that the photocatalytic degradation of methyl orange was 87% when the reaction temperature was kept at 120 °C and the reaction was for three hours[14]. In the year 2018, Ye *et al*., did the comparative study of the photocatalytic behaviour of the ZnS nanopartices towards various dyes such as MO(Methyl Orange), MR(Methyl Red), MB (Methylene Blue) and XO (Xylenol Orange). They found that the degradation of MO and MR dyes are more than the MB and XO dyes. They reported that during 120 minutes of degradation time, the degradation rate for ZnS Nanoparticles for MB, XO, MO and MR are 78.41%, 81.22%, 90.90% and 95.10% respectively. They also reported that is due to the reason that ZnS Nanoparticles can easily degrade the -N=N- bonds[15].

For the enhancement of photocatalytic activity of the semiconductor nanomaterials, sometimes, a shell of another semiconductor material is added over the core material. This is because as the size of the materials increases; surface area and the charge transfer efficiency also increase and thereby increases the absorption towards the UV light[16]. The shell material also provides protection to the core material, thereby increasing its catalytic stability[17].

Photocatalytic studies done using core/shell nanocomposites have been reported by various research groups. CdS/ZnS nanocomposites are one of the best examples of core/shell nanocomposite based photocatalyst. In 2014, Soltani *et al*., studied the photocatalytic activity of CdS and ZnS Nanoparticles capped with PVP (Polyvinyl Pyrollidone) towards degradation of methylene blue dye. They reported that the photocatalytic efficiency increases by a factor of about 1.3 times for ZnS Nanoparticles and 3.2 times for CdS Nanoparticles respectively. Moreover they confirmed that when CdS Nanoparticles are coated with a ZnS shell, the efficiency increases by 1.4 times[18]. In 2015, Tang *et al*., synthesized reduced grapheme oxide (RGO) - CdS/ZnS heterostructured nanocomposites and studied the photocatalytic activity of the as prepared CdS/ZnS nanocomposites upon the photodegradation of tetracycline. They reported that the as prepared core/shell nanocomposite can degrade 85% of the tetracycline under visible light irradiation after 60 minutes of irradiation time[19]. Reddy *et al.*[20], in the year 2017 reported that CdS/ZnS core/shell nanocomposites showed excellent photocatalytic behaviour for the degradation of methyl orange. They found that within 90 minutes of irradiation time 90% of MO was degraded[21,22]. Pollutant Rifampin (RF) was removed from an aqueous solution by Soleimani *et al*., in the year 2020 by photodegradation process using CdS/ZnS Nanoparticles as the photocatalyst under the visible light irradiation technique. They confirmed that the best photocatalytic acitivity can be obtained when the moles of CdS nanoparticles was 6 times more than that of ZnS Nanoparticles[23].

Very recently in 2022, kilogram- scale fabrication of CdS/ZnS 1D/2D heterojunctions were performed by Zhang *et al.*, under room temperatures and atmospheric pressure. They found that under visible-light irradiation, photocatalytic H_2 irradiation rate increases up to 14.02 $mmolh^{-1}g^{-1}$; whereas this rate is 10 and 85 times more than those of pristine CdS nanosheets and CdS nanoparticles respectively[24].

In the current year 2023 Khodamorady *et al*., synthesized ZnS/CdS nanocomposites and studied their photocatalytic activity towards the removal of many dyes such as methylene blue, methyl orange *etc*. They confirmed that ZnS/CdS degraded 96.6% methylene blue and 70.9% methyl orange[25] respectively.

In the current work, we have at first synthesized CdS nanoparticles using a chemical precipitation technique and then these nanoparticles have been coated with a layer of ZnS nanomaterial. We have then measured the visible light photocatalytic activity of CdS/ZnS core/shell nanocomposites. The chemical reaction technique used for the synthesis of the nanocomposites, in this work is simple, efficient, affordable and also ecologically benign, which may produce flawless nanocrystals with high purity. Also in this reaction, we have used a water dispersible polymer; polyvinyl alcohol (PVA), as the matrix material. The entire synthesis process has been carried out in a one-pot reaction. The photocatalytic performance of the CdS/ZnS nanocomposite has been tested for the degradation of Methyl Orange dye. We have therefore attempted to produce improvement in visible light photocatalytic activity of chemically synthesized CdS/ ZnS nanocomposites using PVA as the capping agent throughout the reaction process.

2. Experimental Details

2.1 Materials

All the chemicals viz. Cadmium Chloride ($CdCl_2$), Sodium Sulphide (Na_2S), Zinc Chloride ($ZnCl_2$) and Polyvinyl Alcohol (PVA) were of analytical grade with 99.99 % purity and were all purchased from Sigma-Aldrich/Merck and were directly used without further purification. Double distilled water was used as the solvent throughout the synthesis process.

2.2 Experimental Methods Adopted

In this work, Cadmium Sulphide (CdS) nanoparticles have been synthesized using a simple wet chemical method involving a reaction between the solutions of Cadmium Chloride ($CdCl_2$) and Sodium Sulphide (Na_2S). Polyvinyl alcohol (PVA) has been used as the capping agent throughout the reaction. At first 1 gm of PVA was mixed in 100 ml distilled water. The solution was then magnetically stirred for three hours until it becomes clear. Then, solution of 1gm of $CdCl_2$ and 1 gm of Na_2S were separately prepared by stirring for about half an hour in 100 ml distilled water. After that, solutions of PVA and $CdCl_2$ were mixed in the ratio of (PVA): ($CdCl_2$) = 2:1. To this solution Na_2S was added dropwise, under constant magnetic stirring and the colour change was observed until it turns into yellow from orange, indicating the formation of CdS nanoparticles.

To grow the shell of ZnS nanomaterial over the CdS core nanoparticles, separately $ZnCl_2$ and Na_2S solutions were prepared in 100 ml distilled water. Na_2S was added dropwise to the solution of $ZnCl_2$ under constant magnetic stirring. Finally the prepared ZnS sample was added dropwise to the previously formed solution of CdS nanoparticles at a temperature 60-80 °C, under constant magnetic stirring which resulted in the growth of the ZnS shell over the CdS core, thereby forming CdS/ZnS core/shell nanocomposite.

In the present work, therefore, we have synthesized CdS/ZnS core/shell nanocomposite embedded in PVA matrix. It is known that, the separation of charge carriers in a coupled semiconductor system is a process of reduction and oxidation and as such selection of semiconductors with matched potential positions is very important. There are many reported works, where photodegradation of organic dyes have been carried out utilizing metal oxide semiconductors as the photocatalyst. Such synthesis methods commonly need high temperature calcinations. In contrast, metal sulphides can be commonly synthesized in ambient conditions. Also, metal sulfides have very low water solubility that reduces the leaching of metal cations as the second pollutant agents[26]. Thus, we have selected the CdS/ZnS core/shell system as the photocatalyst in the present work. Details of the synthesized samples are listed in Table 1.

2.3 Photodegradation Experiment

The photocatalytic activity of the prepared sample was evaluated by the degradation of Methyl Orange dye. Photocatalysis experiments were carried out in a regular 50 ml beaker. A laboratory constructed irradiation system equipped with a standard 11watt UV lamp tube was used which was isolated from external light sources. Aqueous solutions (1ppm) of the dye (25 ml) were photolyzed in the presence of the prepared sample, under magnetic stirring. A

Table 1 — Details of the synthesized CdS/ZnS sample

Sample Name	Sample Code	Reaction time (hr)	Concentration of the precursors (gm)		
			$CdCl_2$	$ZnCl_2$	Na_2S
CdS	C1	1	1	1	1
ZnS	Z1	1	1	1	1
CdS/ZnS	C1Z1	3	1	1	1

reaction time of 30 min of stirring in the dark was initiated before the tests to ensure the adsorption and desorption equilibrium between the photocatalyst, water and the dye. 3 ml of the suspension was collected at irradiation time interval of 5 min and centrifuged to remove any stray catalyst powder and their absorbance was recorded by UV visible Spectroscopy. At first, the dye solutions were irradiated without the sample for reference and it was confirmed that the dyes were not decomposed after irradiation for a long time.

Degradation efficiency was estimated using the following equation[23]:

$$\text{Degradation \%} = \left(\frac{A_0 - A_t}{A_0}\right) \times 100 \; or \; \left(\frac{C_0 - C}{C_0}\right) \times 100 \quad \ldots(1)$$

Where, 'C_0' and 'C' are the concentrations of the dye at time *t=0* and at time 't' respectively. A_0 and 'A_t' are the absorbance at time t=0 and at time t respectively.

3 Characterization

The synthesized samples were characterized using different characterization techniques. UV-visible spectra were analyzed using UV-visible spectrophotometer (HITACH Model U-3210). The room temperature photoluminescence spectra were measured using Hitachi F-2500 Photoluminescence spectrophotometer with excitation wavelength 300 nm. X-ray diffraction patterns were recorded with Philips X-ray Diffractometer with CuK_α radiation (λ=1.546A°) in terms of intensity versus 2θ plots with 2θ ranging from 8°-100°. The SEM images of the synthesized samples were recorded with Scanning Electron Microscope [Model no Sigma 300]. Moreover to study the presence of elements in the sample, EDAX analysis was also performed. Transmission Electron Microscope (TEM) and High Resolution Transverse Electron Microscope (HRTEM) images were recorded using TEM [Model JEM 2100].

4 Results and Discussion

4.1 Structural Analysis

X- ray diffraction pattern of the synthesized CdS and CdS/ZnS samples are shown in Fig. 1. The diffraction peaks for the CdS nanoparticles indicates formation of mixed phase of CdS with peaks corresponding to both cubic and hexagonal phases being present in the pattern. Diffraction peaks

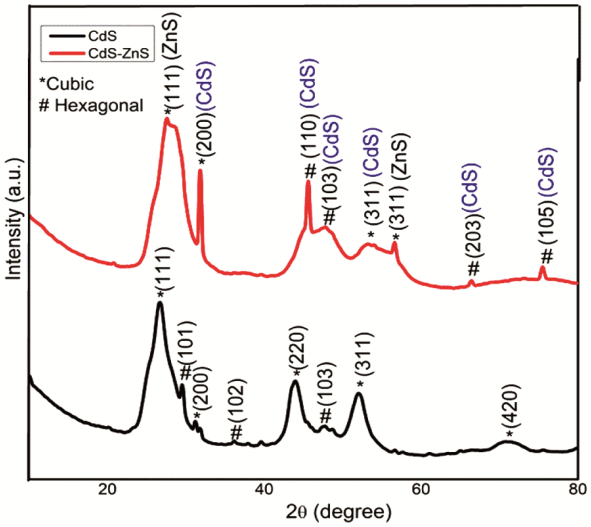

Fig. 1 — XRD pattern of CdS (C1) and CdS/ZnS (C1Z1)

obtained at 2 Theta values of 26.67°, 31.45° , 43.80°, 52.18°, 71.41° corresponds to the reflection planes (111), (200), (220), (311) and (420) respectively which corresponds to the cubic phase of synthesized CdS samples [JCPDS card No 42-1411][20,27]. Diffraction peaks corresponding to 2 Theta values of 28.60°, 36.30° and 47.52° are corresponding to the reflection planes (101), (102) and (103) respectively which shows the hexagonal phase of CdS nanoparticles [JCPDS card No 77-2306][18]. These peaks are less intense; indicating that the cubic phase is more prominent in the synthesized sample. Similar result of formation of mixed phase of CdS was reported by Haque & Sheng *et al.*,[28,29]. The average crystallite size of the samples was calculated using the De-bye Scherrer's formula[30] which is:

$$D = \frac{K\lambda}{\beta Cos\theta} \quad \ldots(2)$$

where β is the full-width at half maximum (FWHM) of a diffraction peak, K = 0.9, θ is the Bragg's angle and λ is the wavelength (=1.54A°) of CuK_α radiation.

For the CdS/ZnS, core/shell composite sample, the reflections corresponding to the cubic phase of CdS nanoparticles are obtained at 2 Theta angles of 31.68° and 52.34° corresponding to (200) and (311) planes respectively; whereas the reflections corresponding to the hexagonal phase are obtained at 2 Theta angles of 45.03°, 47.82°, 66.57° and 75.41° corresponding to (110), (103), (203) and (105) planes of the hexagonal phase of CdS Nanoparticles[18,31]. This confirms the presence of mixed phase (cubic and hexagonal) of

CdS nanoparticles in the composite sample also. Moreover the reflections for ZnS nanoparticles present in the CdS/ZnS nanocomposites are obtained at 2 Theta angles = 28.09° and 56.68° corresponding to the planes (111) and (311) respectively which shows the cubic zinc blende phase of ZnS samples [JCPDS card No 05-0566][18,32]. Similar results were reported by Zhiyuan *et al*., in the year 2018[33]. It is observed that some of the reflections corresponding to CdS Nanoparticles of the CdS/ZnS nanocomposites are shifted towards higher angles due to composite formation. These results confirm the deposition of ZnS shell over the CdS core.

The average crystallite size of CdS Nanoparticles was found to be 11.52 nm which was calculated using Eq. 1 and average crystallite size of CdS/ZnS core/shell nanocomposite was calculated using the same equation and was found to be 16.10 nm, which confirms the deposition of the shell material over the core material, and thereby confirms the formation of CdS/ZnS core/shell nanocomposite.

It is observed that the main diffraction peak is broad for the composite sample in comparison to the core sample. This

may be attributed to the formation of very fine size of grains for the composite sample as compared to the core sample[27]. Further the lattice mismatch between CdS and ZnS across their interface also induces stress and strain, contributing to the broadening[18,34].

4.2 Morphology Study

Figure 2(a) shows the SEM image of the prepared CdS/ZnS core/shell nanocomposite. The image reveals that the particles are more or less spherical in shape. The size of the particles lies in a range of 20-60 nm.

4.3 EDAX Analysis

The Energy Dispersive X-ray Spectroscopy (EDS) image of the as prepared CdS/ZnS samples is shown in the Fig 2(b) below. It provides information regarding the chemical composition of CdS/ZnS nanocomposites. The figure reveals the presence of Cd, S and Zn in the core/shell sample. Other elements like Cl and Ca are also revealed from the EDAX image. This confirms the elemental composition of the sample in thin film form for the analysis. Cl is present in the EDAX analysis as $CdCl_2$ was used as one of the precursors of CdS Nanoparticles. Moreover since the synthesis process is a hydrothermal process so presence of Ca is observed in the EDAX pattern of the CdS/ZnS nanocomposites due to the contamination or the impurities present in the chemical compounds used in the synthesis process[35]. The quantitative elemental composition present in the CdS/ZnS sample is shown in the following Table 2.

4.4 Transmission Electron Microscopy Results

To check the effectiveness of the capping agent and to estimate the particle size of the CdS/ZnS core/shell nanocomposites TEM analysis has been performed. The following figures, Fig. 3(a-f) shows the TEM, HRTEM and SAED pattern of the sample. TEM images of the synthesized CdS/ZnS nanoparticles reveal that, the particles are more or less spherical in

Table 2 — Quantitative elemental composition of CdS/ZnS sample

Element	Weight % Atomic %
S K	18.78 28.18
Cl K	24.99 34.04
Cd L	16.46 7.07
CaK	2.64 3.18
ZnK	37.13 27.43
Total	100%

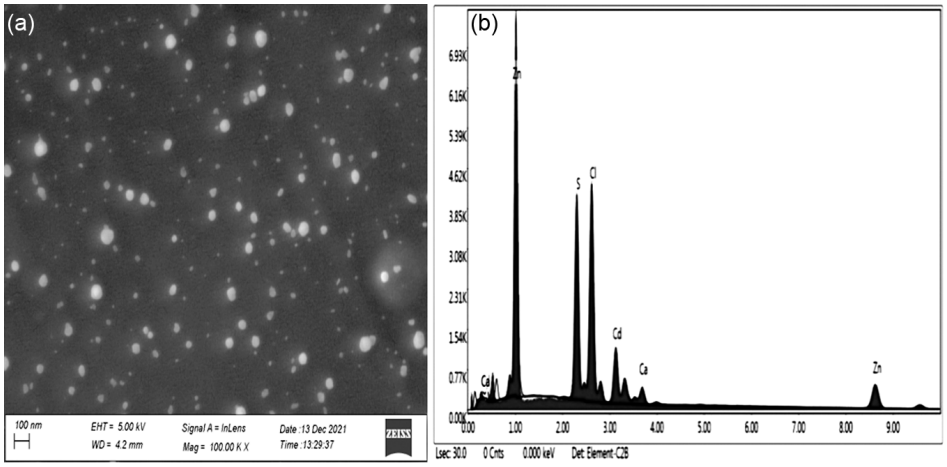

Fig. 2 — (a) SEM image of C1Z1 (b) EDAX image of C1Z1

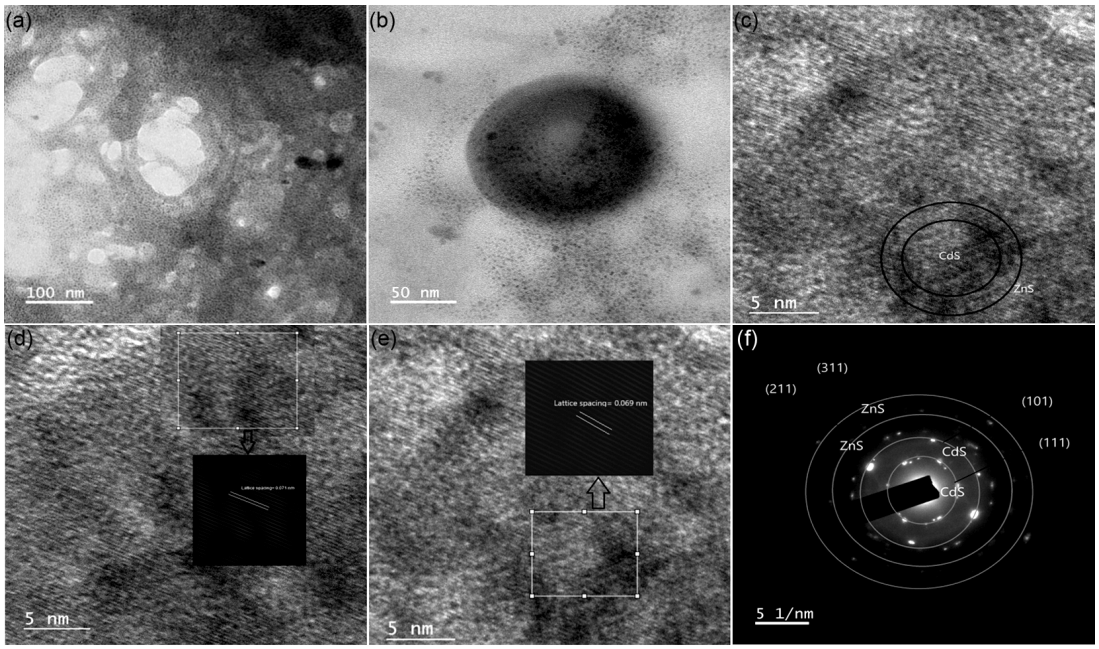

Fig. 3 — (a,b) TEM images of C1Z1 (c) HRTEM image of C1Z1 (d) Lattice spacing of C1 (e) Lattice spacing of Z1 (f) SAED pattern of C1Z1

shape. The TEM images indicate that the produced particles are in the nanometre scale and most of which lies in a range of 60-70 nm. The uniform concentric rings corresponding to different Miller indices in the SAED pattern confirms that the synthesized CdS/ZnS Nanocomposites are highly crystalline which has also been confirmed from the XRD pattern[20].

Figure 3(a) shows the TEM image, from where most of the particles are observed to be almost spherical with the particles lying in the range of 50-60 nm. Fig. 3(b) shows one bigger sized particle with the shell distinctly visible around the core. Fig. 3(c-e) show the HRTEM images of the synthesized particles with the lattice fringes corresponding to different orientations for the core and the shell material being clearly visible. The lattice spacing for the core CdS Nanoparticles was found to be 0.071 nm and for the ZnS shell nanopartices the lattice spacing was found to be 0.069 nm respectively. Fig. 3(f) shows the formation of concentric SAED rings corresponding to both the core and the shell material which shows that the synthesized material is highly crystalline which is in accordance with the XRD results.

4.5 Results of UV-visible Spectroscopy

4.5.1 UV-Vis absorption spectra of the synthesized samples and Tauc's plots corresponding to each sample are shown in the Fig. 4(a,b) below. The absorption edge of CdS sample was found to be at 360.00 nm, which shows a clear blue shift from it's bulk value which is 512 nm[36], indicating the formation of nanoparticles of CdS. The energy band gap value for CdS nanoparticle has been estimated using the Tauc's relation given by the equation[37],

$$\alpha h\nu = (h\nu - E_g)^n \quad \ldots (3)$$

Here, α is the absorption coefficient, hν is the energy of the incident light, E_g = Energy band gap of the material, the value of n depends upon the nature of the transition. For direct and indirect transitions it is ½ and 2 respectively. The band gap value for CdS nanoparticles was calculated and found to be 3.50 eV which is larger than the band gap value of bulk CdS which is 2.42 eV, thereby, also confirming the formation of nanoparticles of CdS. The absorption spectra and Tauc's plot of the CdS, ZnS and CdS/ZnS sample are shown as in Fig. 4(a-c) respectively, while the positions of absorption edges and the corresponding band gap value are listed in Table 3. Moreover the decrease in band gap of CdS/ZnS sample than that of CdS and ZnS nanoparticles confirms the formation of CdS/ZnS core/shell nanoparticles successfully.

Similarly the absorption edge of ZnS sample was found to be at 304.12 nm, which shows a clear blue shift from it's bulk value which is 340 nm. The band gap was found to be 4.10 eV which is larger than that of the the bulk ZnS materials which is 3.68 eV. This indicates the formation of ZnS nanoparticles.

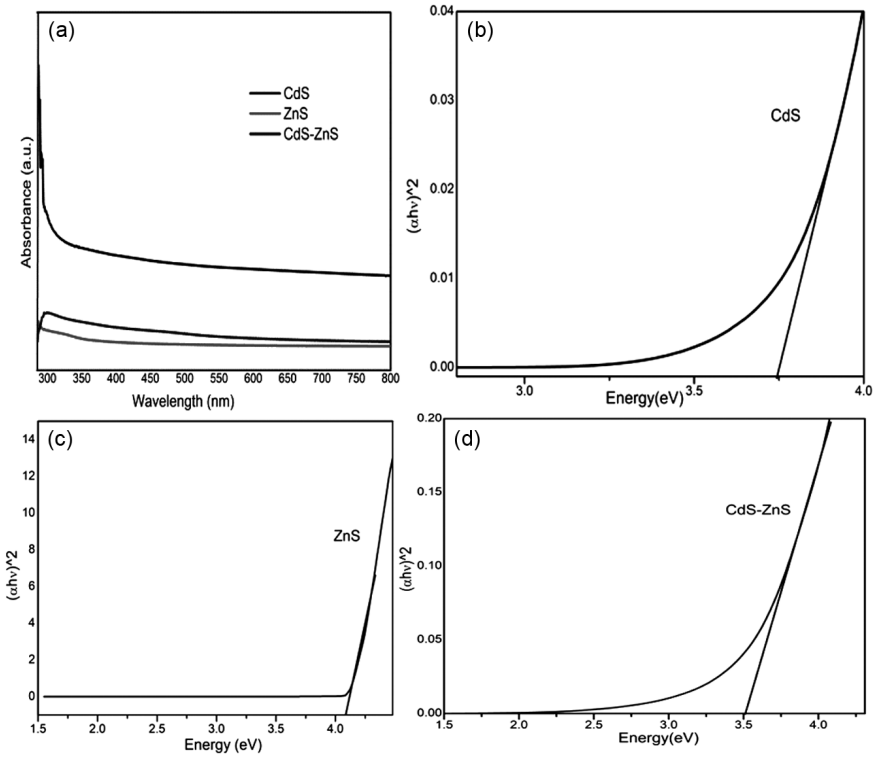

Fig. 4 — (a) Absorption spectra of all samples (b) Tauc's plot of C1 (c) Tauc's plot of Z1 (d) Tauc's plot of C1Z1

Table 3 — Position of absorption edges and band gap values for all the synthesized samples

Sl. No.	Name of the samples	Sample Code	Position of Absorption Edge of samples(nm)	Band Gap of Core/ Shell Samples (eV)
1	CdS	C1	407.91	3.75
2	ZnS	Z1	446.82	4.10
3	CdS/ZnS	C1Z1	494.66	3.50

For the CdS/ZnS nanocomposites, there is a red shifting[20] of the absorption edge compared to the core CdS nanoparticles. The absorption edge is observed at 494.66 nm and as such, the band gap value of the composite sample is lesser than the core CdS nanoparticles, which in turn confirms the deposition of the shell material over the core material, as growing of the shell has resulted in increase of the particle size[38].

4.5.2 Particle size calculation of CdS and CdS/ZnS Nanoparticles using Brus' equation

The diameter of the core CdS nanoparticles has been calculated from the UV data using the Brus' equation given below[39]:

$$E = E_{bulk} + \frac{h^2}{8R^2}\left(\frac{1}{m_e} + \frac{1}{m_h}\right) - \frac{1.8e^2}{4\pi\epsilon R\epsilon_0} \quad \ldots(4)$$

$E_{bulk} = 2.42\ eV\ for\ CdS$, m_e = 0.19 m_0, m_h= 0.8m_0 where m_0 is the rest mass of the electron, m_e and m_h are the masses of electron and hole respectively, R is the radius of the particle and ϵ= 5.7 is the dielectric constant.

The particle diameter 2R was found to be 5.00nm, which is also the particle size.

4.6 Results of Photoluminescence Spectroscopy

Photoluminescence Spectroscopy is a useful characterization technique which provides information about the optical and photochemical characteristics of a semiconductor. The room temperature photo-luminescence spectra of CdS, ZnS and CdS/ZnS samples are shown in Fig. 5 below. The excitation wavelength of CdS, ZnS and CdS/ZnS nanoparticles was 290 nm. The excitonic peak for CdS nanoparticles was located at around 323.23 nm. Similarly for ZnS and CdS/ZnS nanoparticles the excitonic emission peaks are obtained at 323.54 nm and 322.28 nm respectively. From the figure it is observed that CdS sample showed blue emission peaks at 404.15 nm and a shoulder at

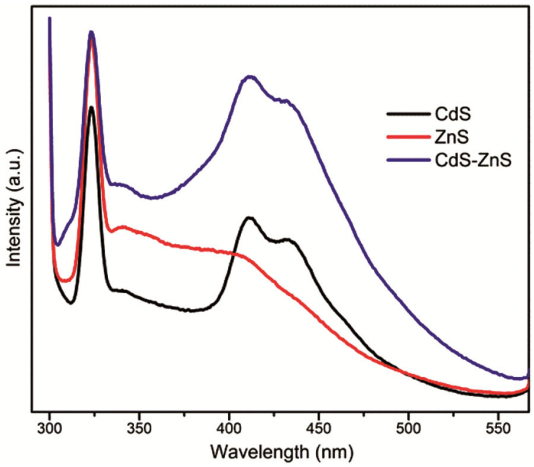

Fig. 5 — Photoluminescence spectra of C1, Z1 and C1Z1

Table 4 — Position of excitonic emission peaks for CdS core and CdS/ZnS core/shell samples

Serial No	Sample Name	Sample Code	Position of Excitonic Emission (nm)
1	CdS	C1	323.23
2	ZnS	Z1	323.54
3	CdS/ZnS	C1Z1	322.28

444.62 nm. This may be attributed to the recombination of trap charge carriers at the surface defects due to Cd and S vacancies[40]. Similar result was reported by Mandal *et al*., for CdS sample[41]. The ZnS sample did not show any significant emission apart from the excitonic emission. The composite CdS/ZnS sample showed a blue emission at 413.75 nm and a shoulder at 441.50 nm. This may be present due to the recombination of trap charge carriers at the surface defects of CdS/ZnS sample. It is observed that, the photoluminescence intensity of the core/shell composite sample of CdS/ZnS is more in comparison to the bare core CdS or shell ZnS nanoparticles. This may be attributed to an increase in the number of radiative transitions caused due to the deposition of ZnS shell nanoparticles over the core CdS nanoparticles. The blue shift in the position of the excitonic emission of the composite can be associated to the presence of ZnS disordered shell material over the surface of the core CdS. The inter band connection at the interface of core CdS and disordered ZnS shell results in the confinement of the photogenerated electron-hole pairs to the interface of the core, due to the effect of quantum confinement. This leads to the passivation of non radiative transition; thereby increasing the number of radiative transitions which leads to an increase in the photoluminescence intensity[42,43]. Positions of excitonic emissions of all samples are listed in Table 4.

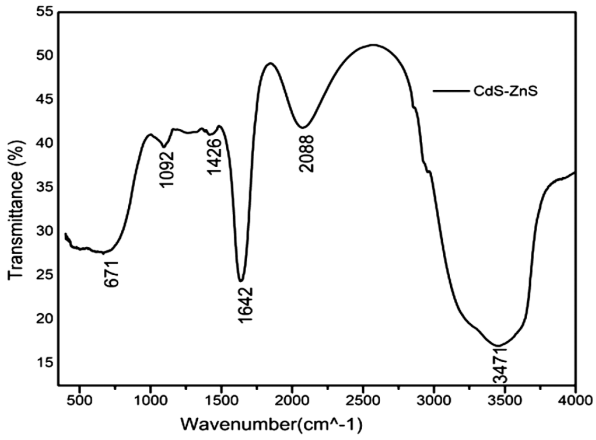

Fig. 6 — FTIR spectrum of C1Z1

4.7 FTIR Analysis

FT-IR spectroscopy has been used to evaluate the chemical bonds of the synthesized CdS/ZnS Nanoparticles and also to identify the organic species used in the synthesis process present in the sample. The obtained spectra are shown in the above Fig. 6. The peaks observed at 671 cm^{-1} indicates the presence of Cd-S bond[44] and that at 1426 cm^{-1} indicate the presence of Zn-S bond[20]. The strong band near 3438 cm^{-1} indicates the presence of hydroxyl group[45]. 1642 cm^{-1} is assigned to O-H stretching vibration of H_2O molecules[46] and 1092 cm^{-1} correspond to Cd-S bond and it indicates the vibrational mode of the sulphide ions in the crystal[47]. The band at 2088 cm^{-1} is due to the O-H bonding of water.

5. Photocatalytic Studies

The photocatalytic activity of the as synthesized CdS/ZnS core/shell nanocomposites, have been studied on the degradation of Methyl Orange organic dye under UV light irradiation. A calculated amount of the sample is added to the Methyl Orange solution in dark condition, and before irradiation, the mixture solution was magnetically stirred in the dark for 30 minutes so as to observe the adsorption-desorption equilibrium between the sample and methyl orange. Before irradiating the sample with the UV-light, the optical absorption spectra have been recorded. After that, the dye-sample mixture solution was kept under irradiation, and the degradation of the dye was observed by measuring the intensity of the absorption peak of the dye at regular intervals. The characteristics absorption peak of Methyl Orange at 450 nm was chosen to monitor its degradation. It was observed that, as irradiation time increased the

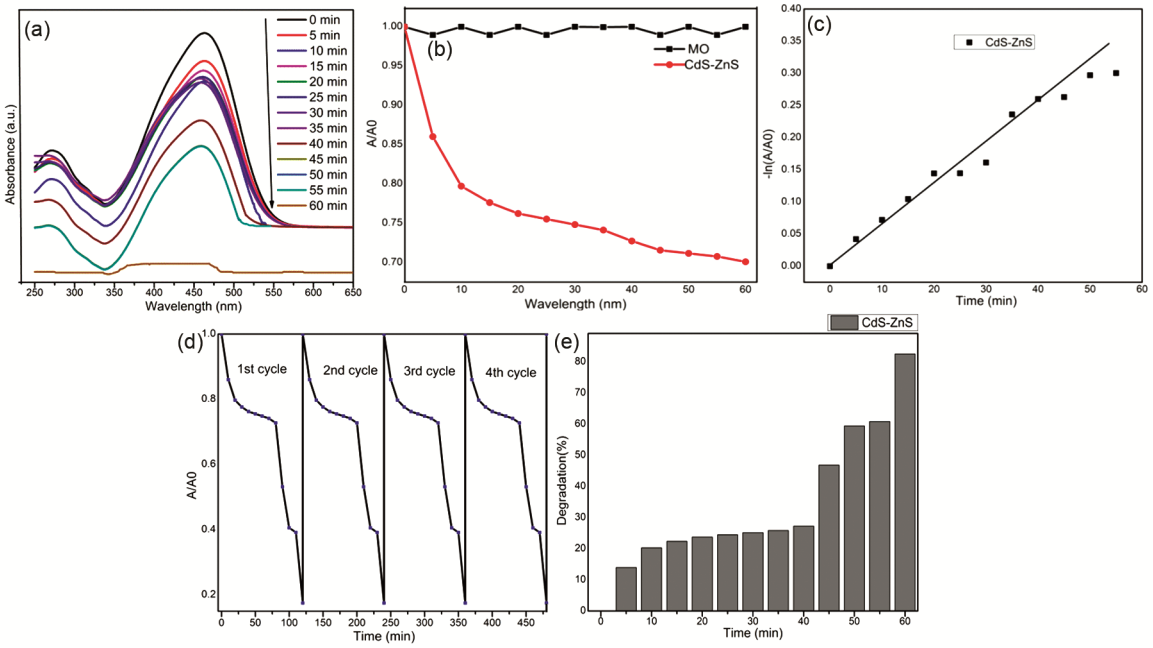

Fig. 7 — (a) Time dependent absorption spectra (b) Photodegradation rate of MO (c) Kinetic plot of photocatalytic activity of MO (d) Recyclability of MO photocatalyst (e) Photodegradation rate of MO photocatalyst

absorption band due to MO gets quenched slowly, and absorption band was almost faded after 60 minutes of irradiation which indicates the discolouration of MO. Thus the CdS/ZnS core/shell composite nanoparticles has acted as a good photocatalyst, and have completely degraded the dye. This is illustrated in Fig. 7(a).

To describe the photo-degradation kinetic behaviour as discussed above, Langmuire-Hinshelwood kinetic equation has been used.

$$r = -\frac{dc}{dt} = Kkc/\,(1 + KC) \qquad \ldots(5)$$

where, r and c represent the rate of the reaction (mol $L^{-1}min^{-1}$) and equilibrium constant (mol L^{-1}) of the reagent respectively; t signifies time; K and k represents Langmuir constant (L mol^{-1}) and rate constant (L min^{-1}) respectively[48]. From the slope of the function of the irradiation time, the degradation constants are calculated[49]. The evaluated degradation rate constant for CdS/ZnS Nanoparticles is found to be 0.003956 min^{-1}. Fig. 7(a) indicates the absorption spectra at zero time for blank MO and at different irradiation times for the MO-photocatalyst mixture solution. The photocatalytic degradation of the MO dye in presence of CdS/ZnS nanocomposite as the photocatalyst under the irradiation of UV light, is observed from the figure.

As shown in the Fig. 7(b) a blank experiment for degradation has been carried out for MO in the absence of photocatalyst under visible light irradiation. No degradation of MO has been observed during this experiment. The degradation of MO was observed when we added CdS/ZnS nanocomposite sample with it and recorded the corresponding optical absorption spectra under UV light with the time. It was also observed that, the degradation of MO increases as the time increases. The efficiency of degradation was calculated using Eq. 1 and found to be up to 82.5% at the time 60 minutes. Hence it is confirmed that CdS/ZnS nanocomposites can act as a good photocatalyst to degrade the MO dye. Fig. 7(c) shows the kinetic plot of photocatalytic activity of MO. The result of cyclic photodegradation tests are repeated in four cycles as shown in Fig. 7(d). It was observed that there was no any noticeable degradation in photocatalytic activity after the four repetitive cycles. The above result concludes that the synthesized CdS/ZnS core/shell composite photocatalyst is stable. Fig. 7(e) shows the percentage of degradation of the dye at different time intervals.

6 Mechanism of Photocatalytic Activity

The photocatalytic activity of CdS/ZnS nanocomposites is based on the mechanism of the photogenerated electrons and holes. CdS/ZnS

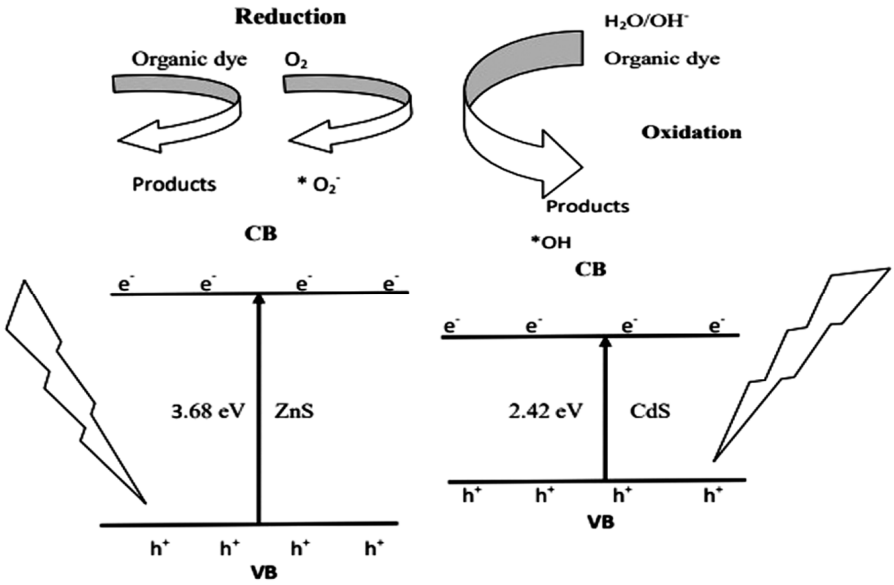

Fig. 8 — Photocatalytic mechanism in CdS/ZnS nanocomposite

core/shell nanocomposites are able to exhibit increased photocatalytic performance due to several reasons which include: presence of defect sites at CdS/ZnS core/shell interface, the intimate connection between CdS and ZnS and the high surface-to-volume ratio. The charge separation mechanism in core/shell semiconductor based photocatalysts is a process that involves the transfer of photogenerated charges from one semiconductor into the lower lying energy bands of another. In this case, the photo-generated electron (e-) and hole (h+) pairs are responsible for the increased photocatalytic activity of CdS/ZnS core/shell composite nanoparticles. When the UV light illuminates the sample mixture, photoexcited electron-hole pairs are created ((equations (a) and (b)). All photogenerated electrons and holes are consequently transferred to the conduction band (CB) and valence band (VB) of CdS respectively based on the position of the respective energy band levels ((equation (c)). In the oxygen equilibrated media, the photo-excited electrons are scavenged by molecular oxygen O_2 to hydrogen peroxide H_2O_2 ((equation (e)) and the superoxide radical anion O^2– (equation (d)). H_2O_2 and O_2^- produces the hydroxyl group OH ((equation (f)). OH is an oxidized species and thereby degrades the dye molecule ((equation (g)). Moreover these intermediate radicals degrade the dye molecule of MO. Since due to the valance band potential the photogenerated holes in CdS cannot participate in the oxidation of hydroxyl group thereby results in the photo-corrosion of CdS and as a result Cd ions are produced ((equation (h))[50,51].

Due to the wider band gap of ZnS shell material, in the CdS/ZnS core/shell nanomaterial; both the energy levels (conduction band and valence band) of ZnS are displaced symmetrically from the band gap of the core material. Moreover when the shell material is excited both the outer electrons and holes get relaxed into the core material. For the enhanced photocatalytic activity of the CdS/ZnS nanocomposites, three phenomenon are responsible, which are: (i) the shell material effectively passivate the surface electron states of the CdS core (ii) surface charge modification, inhibition of CdS photo-corrosion and surface electronic state passivation of CdS core material due to the presence of ZnS shell material and (iii) since ZnS is a wide band gap semiconductor, its band gap energy provides the required potential energy to restrict both electrons and holes inside the band gap of the CdS core material[52]. The mechanism of photocatalytic degradation is illustrated in Fig. 8 above. The whole reactions involved in the mechanism can be expressed as follows[53].

$CdS/ZnS \rightarrow^{h\upsilon} CdS(e^- + h^+)/ ZnS$ ...(a)

$CdS/ZnS \rightarrow^{h\upsilon} CdS/ZnS\ (e^- + h^+)$ ...(b)

$CdS/ZnS\ (e^- + h^+) \rightarrow CdS(e^- + h^+)/ ZnS$ ...(c)

$CdS(e^- + h^+)/ ZnS + O_2 \rightarrow CdS(h^+)/ZnS + O_2$- ...(d)

$CdS(e^- + h^+)/ZnS + O_2 + 2H^+ \rightarrow CdS(H^+)/ ZnS + H_2O_2$ ...(e)

$H_2O_2 + O_2^- \rightarrow OH + OH^- + O_2$ ...(f)

$OH + dye \rightarrow$ degradation products ...(g)

$CdS(e^- + h^+)/ZnS + dye \rightarrow CdS(e^-)/ZnS + dye$
$\rightarrow CdS(e^-)/ZnS +$ degradation products ...(h)

7 Conclusion

CdS and ZnS nanoparticles and CdS/ZnS core/shell nanocomposite are successfully synthesized using chemical precipitation technique. From the XRD results, it is confirmed that the synthesized CdS and ZnS nanoparticles are of face centred cubic phase. The presence of C-S and Zn-S bonds is confirmed from the FTIR analysis of the core/ shell nanocomposites. Moreover the elemental compositions are confirmed from the EDAX analysis of CdS/ZnS nanocomposite. The optical absorption spectra of CdS/ZnS core/shell nanocomposites showed that the absorption edges are blue shifted compared to the corresponding bulk material. The photocatalytic degradation of methyl orange in presence of CdS/ZnS nanocomposite photocatalyst has been successfully studied. It has shown that the photodegradation of methyl orange increases as the degradation time increases. Thus, we can confirm that the CdS/ZnS core/shell nanocomposite is a good photocatalyst. The synthesized CdS/ZnS core/shell composite nanoparticles also showed better stability for repetitive use as a photocatalyst.

Acknowledgement

The authors sincerely acknowledge the Department of Chemistry, Gauhati University for their help in availing the SEM and EDAX facilities, the Department of Instrumentation and USIC, Gauhati University for XRD facility and CIF, IIT Guwahati for providing the TEM/HRTEM analysis of the samples. The first author (Pallabi Boro) also acknowledges CSIR, New Delhi for the financial support under JRF scheme [File no-09/059(0066)/2018-EMR-I, date: 22/02/2019].

References

1 Rajbongshi H, Bhattacharjee S & Dutta P, *Mater Res Express*, 6 (2019) 045022.
2 Kaur S, *Int J Eng Appl Sci Technol*, 2 (2017) 75.
3 https://www.sciencedirect.com/topics/materials-science/homogeneous-photocatalysis
4 Šuligoj A, Korošec R C, Žerjav G, Tušar N N & Stangar U L, *Top Curr Chem(Z)*, 380 (2022).
5 Uchil J & Pattabi M, *J New Mat Electrochem Syst*, 8 (2005) 155.
6 Asthaputre S S, Deshpande A, Marathe S, Wankhede M E, Chimanpure J, Pasricha R, Urban J, Haram S K, Gosavi S W & Kulkarni S K, *Pramana J Phys,* 65 (2005) 615.
7 Wang R, Xu D, Liu J, Li K & Wang H, *Chem Eng J,* 168 (2011) 455.
8 Zhang H, Wei B, Zhu L, Yu J, Sun W & Xu L, *Appl Surf Sci,* 270 (2013) 133.
9 Yu Y, Ding Y, Zuo S & Liu J, *Int J Photoenergy,* 2011 (2011) 762929.
10 Chen F, Cao Y, Jia D & Niu X, *Ceram Int*, 39 (2013) 1511.
11 Bhadwal A S, Tripathi R M, Gupta R K, Kumar N, Singh R P & Shrivastav A, *R Soc Chem,* 4 (2014) 9484.
12 Luo M, Liu Y, Hu J, Liu J & Richards R M, *Appl Catal B: Environ*, 125 (2012) 180.
13 Yin L, Wang D, Huang J, Cao L, Ouyang H & Yong X, *J Alloys Compd,* 664 (2016) 476.
14 Chanu T I, Samanta D, Tiwari A & Chatterjee S, *Appl Surf Sci*, 391 (2016) 548.
15 Ye Z, Kong L, Chen F, Chen Z, Lin Y & Liu C, *Optik*, 164 (2018) 345.
16 Rajbongshi H & Kalita D, *J Nanosci Nanotechnol*, 20 (2020) 5885.
17 Wang X, He B, Hu Z, Zeng Z & Han S, *Sci Technol Adv Mater,* 15 (2014) 043502.
18 Soltani N, Saion E, Yunus W M M, Erfani M, Navasery M, Bahmanrokh G & Razaee K, *Appl Surf Sci*, 30 (2014) 440.
19 Tang Y, Liu X, Ma C, Zhou M, Huo P, Yu L, Pan J, Shi W & Yan Y, *New J Chem*, 39 (2015) 5150.
20 Reddy C V, Shim J & Cho M, *J Phys Chem Solids*, 103 (2017) 209.
21 Vattikuti S V P, Byon C & Reddy C V, *Microst*, 85 (2015) 124.
22 Devaraji P, Sathu N K & Gopinath C S, *ACS Catal,* 4 (2014) 2844.
23 Soleimani F & Ejhieh A N, *J Mater Res Technol*, 9 (2020) 16237.
24 Zhang D, Teng J, Yang H, Fang Z, Song K, Wang L, Hou H, Lu X, Bowen C R & Yang W, *Carbon Energy Wiley,* 5 (2023) 1.
25 Khodamorady M & Bahrami K, *Sci Rep*, 13 (2023).
26 https://www.sciencedirect.com/topics/engineering/metal-sulfides.
27 Prabhu R R & Khadar M A, *Pramana J Phys*, 65 (2005) 801.
28 Haque S E, Ramdas B, Padmavathy N & Sheela A , *Micro Nano Lett*, 9 (2014) 731.
29 Sheng C K & Alrababah Y M, *Heliyon,* 9 (2023) e15908.
30 Ch A, Rao K V & Chakra C S, *Adv Appl Sci Res*, 5 (2014) 99.
31 Seyghalkar H, Sabet M & Niasari M S, *High Temp Mater Proc,* 35 (2016) 1013.
32 Iranmaneesh P, Saeednia S & Nourpour M, *Chin Phys B,* 24 (2015) 046104.
33 Ye Z, Kong L, Chen F, Chen Z, Lin Y & Liu C, *Optik,* 164 (2018) 345.
34 Soltani N, Saion E, Erfani M, Bahrami A, Navasery M, Rezaee K & Hussain M Z, *Chalcogenide Lett,* 9 (2012) 379.
35 https://en.wikipedia.org/wiki/Contamination.
36 Saravanan L, Diwakar S, Mohankumar R, Pandurangan A & Jayavel R, *Nanomater Nanotechnol,* 1 (2011) 42.
37 Xu X, Lu R, Zhao X, Xu S, Lei X, Zhang F & Evans D G, *Appl Catal B: Environ*, 102 (2011) 147.
38 Kumar H, Barman P B & Singh R R, *Phys E: Low- Dimens Syst Nanostruct*, 67 (2015) 168.
39 Unni C, Philip D, Smitha S L, Nissamudeen K M & Gopchandran K G, *Spectrochim Acta Part A*, 72 (2009) 827.
40 Chestnoy N, Harris T D, Hull R & Brus L E & Chestnoy N, *J Phys Chem,* 90 (1986) 3393.
41 Mandal P, Talwar S S, Srinivasa R S & Major S S, *Appl Phys A,* 94 (2009) 577.

42 Amiri O, Mashkani S M H, Rad M M & Abdvali F *Superlattices Microstruct*, 66 (2014) 67.
43 Wang L, Wei H W, Fan Y J, Liu X Z & Zhan J H, *Nano Scale Res Lett*, 4 (2009) 558.
44 Kumar S & Sharma J K, *Mater Sci- Pol*, 34 (2016) 368.
45 Ayodhya D & Veerabhadram G, *J Sci- Adv Mater Dev*, 4 (2019) 381.
46 Gadalla A, Abd EL-Sadek M S & Hamood R, *Chalcogenide Lett*, 15 (2018) 281.
47 Kumar S, Sharma P & Sharma V, *IEEE T Nanotechnol*, 13 (2014) 343.
48 Motahari F, Mozdianfard M R, Soofivand F & Niasari M S, *RSC Adv,* 4 (2014), 27654.
49 Ge J P & Li Y D, *Adv Funct Mater*, 14 (2004) 157.
50 Wu L, Yu J C & Fu X, *J Mol Catal A: Chem,* 244 (2006) 25.
51 Zyoud A H, Zaatar N, Saadeddin I, Ali C, Park D, Campet G & Hilal H S, *J Hazard Mater,* 173 (2010) 318.
52 Rao C N R, Müller A & Cheetham A K, *The Chemistry of Nano materials*, Wiley VCH, Federal Republic of Germany, 2006.
53 Qutub N, Pirzada B M, Umar K, Mehraj O, Muneer M & Sabir S, *Physica E*, 74 (2015) 74.